Society of Medical Education & Research

2023, Volume 3, Issue 2, Page No: 141-163
ISSN: 3108-4834

Archive of International Journal of Cancer and Allied Science

Deubiquitinase USP10 Drives β-Catenin Stabilization, Stem Cell Identity, and Tumorigenicity in APC-Mutant Colorectal Cancer

Gustavo Henrique Silva[1]*, Renato Luiz Oliveira[1]

[1]Department of Oncology, Hospital AC Camargo Cancer Center, São Paulo, Brazil.

***E-mail** ✉ g.silva.accamargo@yahoo.com

Abstract

The role of deubiquitylating enzymes (DUBs) in maintaining β-Catenin stability in intestinal stem cells and colorectal cancer (CRC) is not well characterized. Using an unbiased screening approach, we identified the DUB USP10 as a stabilizer of β-Catenin specifically in APC-truncated CRC models, both in vitro and in vivo. Mechanistic analyses, including in vitro binding assays and computational modelling, indicated that USP10 interacts with β-Catenin through its unstructured N-terminal region, an interaction that is competitively inhibited by full-length APC, promoting β-Catenin degradation. In contrast, in APC-truncated CRC cells, USP10 binds β-Catenin and enhances its stability, which is critical for preserving an undifferentiated tumor phenotype. Loss of USP10 decreased WNT and stem cell signature gene expression while inducing differentiation markers. Notably, silencing USP10 in both murine and patient-derived CRC organoids demonstrated its necessity for NOTUM signaling and the APC super-competitor phenotype, reducing the tumorigenicity of APC-truncated CRC. Clinically, USP10 dependence in patient-derived organoids correlates with worse CRC prognosis. These results reveal USP10 as a key regulator of CRC cell identity, stemness, and tumor growth through β-Catenin stabilization, resulting in aberrant WNT activity and degradation-resistant tumors, highlighting USP10 as a promising therapeutic target in APC-truncated CRC.

Keywords: Cancer genetics, Ubiquitylation, Stem cell, Colorectal cancer

Introduction

Colorectal cancer (CRC) ranked third in global incidence and accounted for an estimated 8–9% of cancer-related deaths in 2021 [1]. Environmental factors, including diet, obesity, physical inactivity, alcohol, and tobacco consumption, are recognized to elevate CRC risk [2]222. In addition to these, hereditary forms of CRC, driven by specific mutations, occur less frequently [3]. Although overall survival post-diagnosis is generally favorable, only about 10% of patients with advanced disease survive beyond five years [4], emphasizing the need for novel exploitable vulnerabilities in CRC, affecting both sexes, with 8% of new cases estimated.

Approximately 80% of CRC cases show WNT signaling hyperactivation [5], primarily due to truncating mutations in the tumor suppressor gene Adenomatous Polyposis Coli (APC). These truncations impair the WNT destruction complex's ability to degrade β-Catenin, leading to degradation-resistant tumors (DRTs) [5, 6]. Multiple APC "hotspot" mutations, including those in the catenin inhibitory domain (CID), produce various truncation variants observed in patients [7]. The CID contains 20 amino acid repeats (20 AAR) that bind β-Catenin. As a result, APC-truncated tumor cells accumulate β-Catenin, which translocates to the nucleus, displaces TLE co-repressors, and partners with TCF-4/LEF-1 to drive WNT target gene expression [8, 9]. β-Catenin accumulation promotes proliferation independent of WNT ligand and is a key event in CRC initiation [10, 11].

Access this article online https://smerpub.com/

Received: 29 May 2023; **Accepted:** 21 October 2023

How to cite this article: Silva GH, Oliveira RL. Deubiquitinase USP10 Drives β-Catenin Stabilization, Stem Cell Identity, and Tumorigenicity in APC-Mutant Colorectal Cancer. Arch Int J Cancer Allied Sci. 2023;3(2):141-63. https://doi.org/10.51847/Dey7TJvJC4

APC truncations influence β-Catenin levels and activity, driving oncogenic transformation [9, 12–15], as these cells have a limited capacity to ubiquitylate β-Catenin [7]. Despite residual post-translational modification (PTM) activity from truncated APC [7], several E3 ligases, including HUWE1 [16], FBXW7 [17], JADE-1 [18], UBR5 [19], and RNF4 [20], modulate β-Catenin ubiquitylation independently of the WNT destruction complex [21, 22].

Beyond ubiquitin ligases, certain DUBs, such as USP7 [13] and USP20 [23], have been shown to deubiquitinate β-Catenin, fine-tuning its abundance and activity [24]. However, it remains unclear whether APC truncation status affects DUB-mediated β-Catenin stabilization. Truncated APC may not only block normal β-Catenin degradation but also act as a scaffold for DUBs, promoting β-Catenin accumulation specifically in APC-truncated CRC. This raises the possibility that loss of discrete APC domains could create new protein-protein interactions that tumors become reliant on.

In this study, we identified USP10 as a DUB that directly binds β-Catenin. This interaction occurs only in cells lacking all AAR domains of APC, a mutation found in ~30% of CRC patients [25, 26]. USP10 is essential for β-Catenin-driven tumorigenic signaling, enhancing WNT target gene expression and maintaining stemness in CRC and murine organoids. This mechanism is evolutionarily conserved, as USP10 loss suppresses gut progenitor hyperproliferation and reduces survival in homozygous Apc (ApcQ8/Q8) D. melanogaster models [27]. USP10 depletion also curtailed patient-derived organoid growth, dampened WNT and EMT signaling, activated the unfolded stress response, impaired NOTUM signaling [28, 29], and prevented tumor engraftment in vivo.

Overall, these findings demonstrate that USP10 stabilizes β-Catenin, promotes WNT signaling, and preserves cancer stemness, all critical for tumor initiation and progression in an APCΔAAR truncation-dependent manner. Targeting USP10 could represent a promising therapeutic strategy for CRC patients harboring APCΔAAR-truncating mutations.

Results and Discussion

USP10 functions as a novel regulator of β-Catenin signaling in CRC and associates with poor patient prognosis

In colorectal cancer, stabilization of the WNT effector β-Catenin is essential for tumor development and can result from either loss-of-function mutations or truncations in the APC gene, or mutations affecting the degron motif within CTNNB1, which encodes β-Catenin. Although dysregulation or mutation of upstream canonical β-Catenin regulators leads to abnormal WNT target gene expression due to elevated β-Catenin protein levels [24, 30], we sought to determine whether β-Catenin ubiquitylation itself is altered [21], as multiple additional ubiquitin-regulatory mechanisms have been previously implicated in CRC oncogenesis.

To explore whether APC or CTNNB1 mutation status affects β-Catenin stability and ubiquitylation, we performed endogenous ubiquitin TUBE (tandem ubiquitin-binding entity) assays across a panel of human CRC cell lines. These included β-Catenin mutant lines (HCT116 and LS174T) and lines with varying APC truncation lengths: DLD-1, SW480, SW620, Colo320, and HT-29 (**Figure 1a**). Interestingly, poly-ubiquitylation of β-Catenin was detectable regardless of the specific genetic alterations (**Figure 1a**), indicating that β-Catenin stability may be regulated in a UPS-specific manner, potentially influenced by additional factors.

To identify such regulators, we conducted a human DUB siRNA screen in APC-truncated HT-29 cells, assessing endogenous β-Catenin levels via high-content immunofluorescence microscopy 48 hours post-transfection, compared to siRNA control-transfected cells (**Figures 1b and 1c**). The screen not only recovered previously described β-Catenin regulators, such as USP20 and UCHL1, but also revealed USP10 as a novel positive regulator of β-Catenin stability, alongside other identified DUBs (**Figure 1c**). Loss of USP10 significantly reduced both cytosolic and nuclear β-Catenin levels, as confirmed by immunofluorescence **(Figure 1c).**

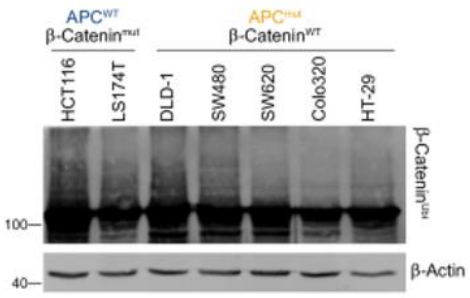
APC^WT
β-Catenin^mut
APC^mut
β-Catenin^WT
HCT116
LS174T
DLD-1
SW480
SW620
Colo320
HT-29
β-Catenin^mut
100
40
β-Actin

a)

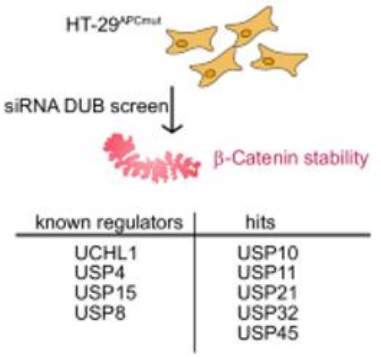
HT-29^APCmut
siRNA DUB screen
β-Catenin stability
known regulators
hits
UCHL1
USP4
USP15
USP8
USP10
USP11
USP21
USP32
USP45

b)

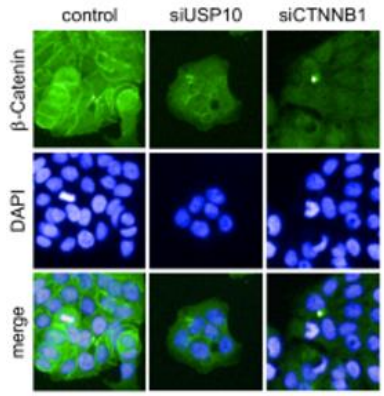
control
siUSP10
siCTNNB1
β-Catenin
DAPI
merge

c)

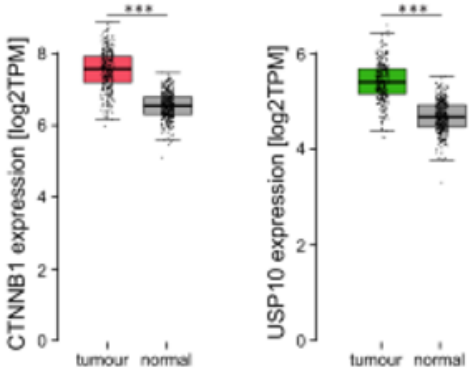
CTNNB1 expression [log2TPM]
USP10 expression [log2TPM]
***
***
tumour
normal
tumour
normal

d)

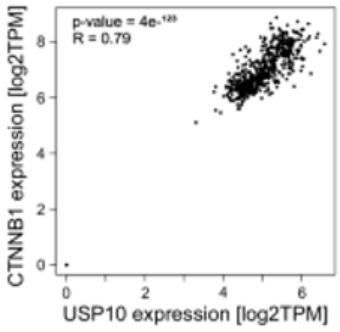
p-value = 4e-123
R = 0.79
CTNNB1 expression [log2TPM]
USP10 expression [log2TPM]

e)

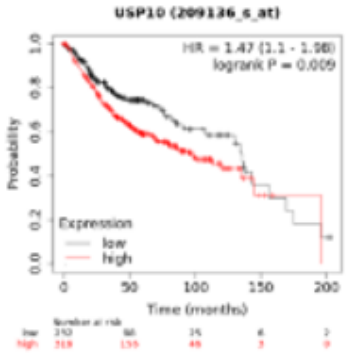
USP10 (209136_s_at)
HR = 1.47 (1.1 - 1.98)
logrank P = 0.009
Probability
Expression
low
high
Time (months)

f)

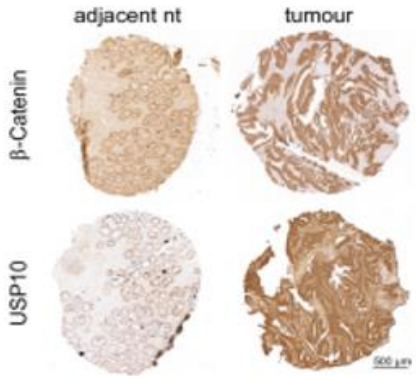
adjacent nt
tumour
β-Catenin
USP10

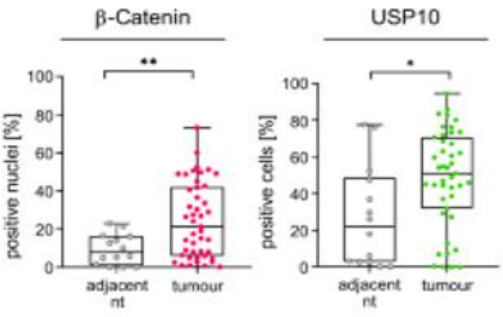
β-Catenin
USP10
**
*
positive nuclei [%]
positive cells [%]
adjacent nt
tumour
adjacent nt
tumour

g)

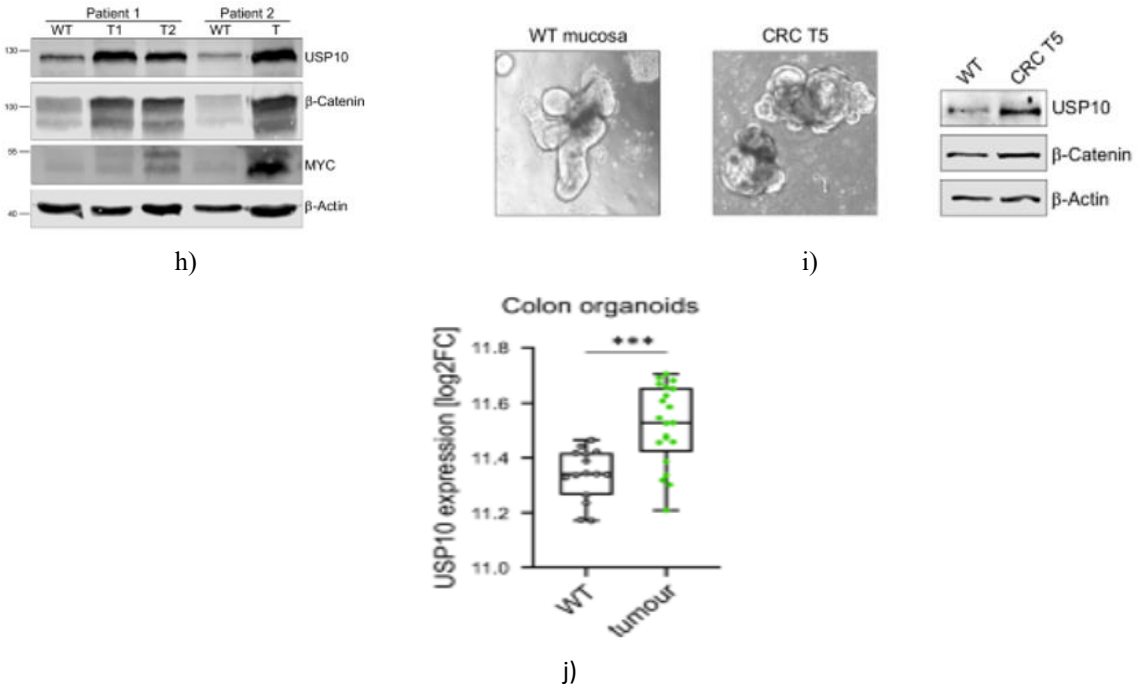

Figure 1. USP10 acts as a novel β-Catenin regulator in CRC and associates with poor patient outcomes**.**

a TUBE assay detecting endogenous poly-ubiquitylated proteins followed by immunoblotting for β-Catenin across human CRC lines with distinct mutations: β-Catenin mutant HCT116 and LS174T; APC mutant DLD-1, SW480, SW620, Colo320, and HT-29. β-Actin was used as a loading control.

b Diagram of the siRNA DUB library screen in APC-mutant HT-29 cells. Four individual siRNAs per DUB were transfected, and 48 h later, endogenous β-Catenin was analyzed via high-content Operetta imaging (n=3). DAPI marks nuclei. Both known and novel regulators were highlighted.

c Representative immunofluorescence of β-Catenin (green) following siRNA knockdown of NTC (control), CTNNB1, or USP10. DAPI (blue) marks nuclei.

d CTNNB1 and USP10 expression in normal vs. CRC tissues, using GEPIA (COAD n=275, GTEx n=349). Boxplots display USP10 and CTNNB1 levels; one-way ANOVA used for p-value calculation. ***p<0.001.

e Correlation analysis of CTNNB1 and USP10 expression in human CRC. R indicates Spearman's coefficient. nT=275, nN=349. Visualization via GEPIA.

f Survival analysis of CRC patients stratified by USP10 expression (low n=206; high n=26), using R2 platform (Tumor Colon - Smith dataset).

g Immunohistochemistry of CRC tissue microarray, showing adjacent non-transformed (adjacent nt) and tumor samples stained for β-Catenin and USP10. Mann–Whitney U test used. *p<0.05; **p<0.005.

h Immunoblot of USP10, β-Catenin, and MYC in non-transformed (WT) and matched CRC tumors (T) from two patients. β-Actin as loading control.

i Brightfield images of patient-derived intestinal organoids (WT mucosa vs. CRC T5). Immunoblots show USP10 and β-Catenin levels; β-Actin is a control.

j USP10 expression in normal (WT) vs. CRC patient-derived organoids, analyzed using R2 (Organoid - Clevers dataset). Mann–Whitney U test applied. ***p<0.001.

Since USP10 had not been previously associated with β-Catenin signaling or intestinal homeostasis, we next explored its expression using publicly available colorectal cancer patient datasets [25]. Although USP10 mutations were uncommon in CRC, the gene was frequently overexpressed alongside CTNNB1 when compared with adjacent non-tumor tissue (**Figures 1d and 1c**). Importantly, USP10 and CTNNB1 expression levels showed a strong positive correlation in CRC samples (**Figure 1e**; nT = 275, nWT = 349, Spearman R = 0.79). Elevated USP10 expression was also strongly linked to worse overall survival among CRC patients (**Figure 1f**), particularly within molecular subtypes CMS2–4 (**Figure 1e**).

Motivated by these findings, we assessed protein levels of USP10 and β-Catenin in CRC tissues using immunohistochemistry (IHC) on tissue microarrays (TMA) containing both tumor and adjacent normal regions. Beyond structural differences between normal and cancerous tissue, USP10 and β-Catenin levels were markedly higher in tumors (**Figure 1g**). This upregulation was further confirmed in human CRC resection samples via immunoblotting, where tumor samples displayed increased USP10, β-Catenin, and the oncogene MYC compared to matched non-transformed tissue (**Figure 1h**).

Analysis of publicly available data revealed that USP10 and CTNNB1 overexpression occur regardless of CRC stage (**Figure 1f**). Single-cell sequencing datasets from two independent studies demonstrated that USP10 expression is specifically elevated in tumor cells relative to normal intestinal cells (**Figure 1g**). Spatial transcriptomics data from a publicly accessible CRC dataset corroborated these findings (https://www.10xgenomics.com/datasets/visium-hd-cytassist-gene-expression-libraries-of-human-crc; **Figure S1** extended). These observations were reproduced in human and murine intestinal organoid models: tumor-derived organoids exhibited higher USP10 protein levels than wild-type counterparts (**Figure 1i**), consistent with patient tumor tissue. Publicly available datasets of patient-derived organoids further validated the increase in USP10 in CRC organoids compared to non-oncogenic organoids [31] (**Figure 1j**). Taken together, these data suggest that USP10 may act as a previously unrecognized regulator of β-Catenin, potentially contributing to WNT pathway activity, intestinal homeostasis, and colorectal tumorigenesis.

USP10 upregulation occurs early in murine models of intestinal cancer

To examine USP10 expression in the intestine, we analyzed its distribution within the intestinal stem cell niche, focusing on unperturbed crypts (**Figures 2a, b and 2a, b**). Fractionation of murine small intestine followed by immunoblotting revealed that USP10 is enriched in crypts relative to villi (**Figure 2a**). Immunofluorescence confirmed this localization and showed nuclear enrichment of USP10 in intestinal stem cells (USP10+/β-Cateninnuclear; USP10+/Cd44high; USP10+/Lysozyme−; **Figures 2b and 2b**). These findings were further supported by publicly available spatial transcriptomic data for murine intestine (https://www.10xgenomics.com/datasets/visium-hd-cytassist-gene-expression-libraries-of-mouse-intestine).

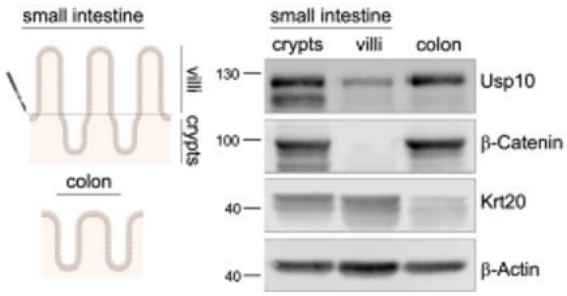

a)

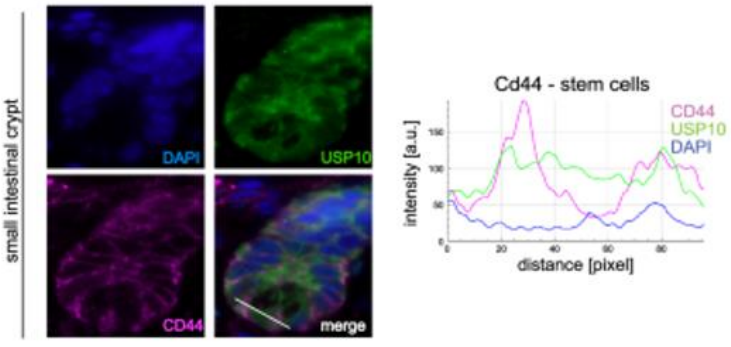

b)

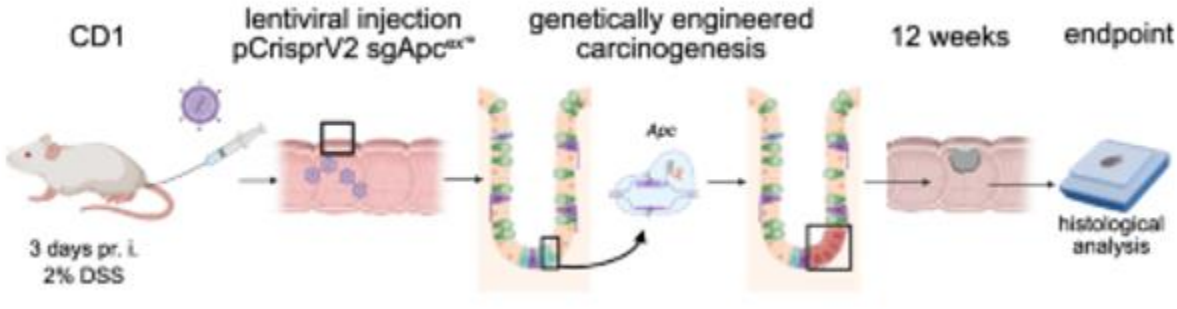
CD1
lentiviral injection
pCrisprV2 sgApc
genetically engineered
carcinogenesis
12 weeks
endpoint
Apc
3 days pr. i.
2% DSS
histological
analysis

c)

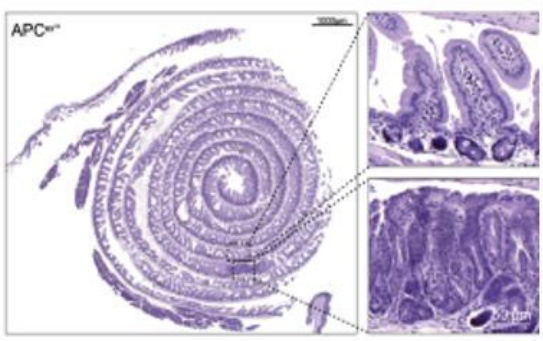

d)

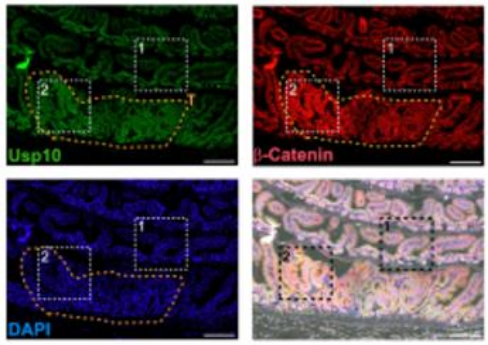
Usp10
β-Catenin
DAPI

e)

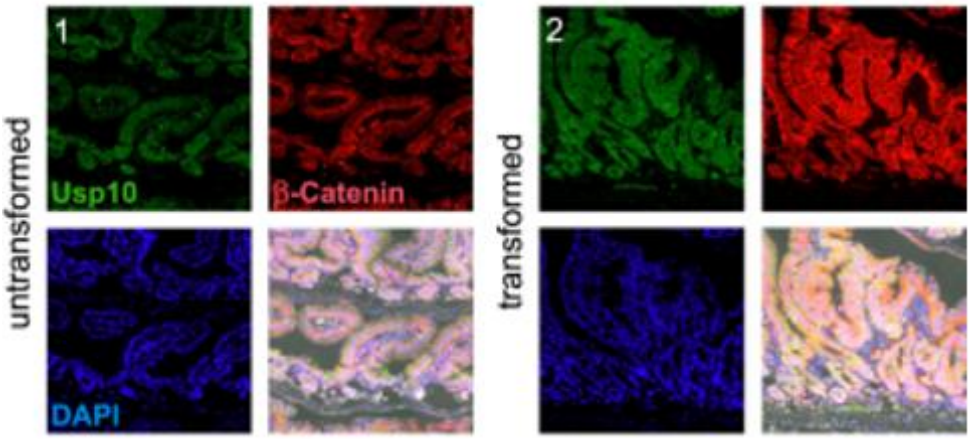
untransformed
transformed
1
2
Usp10
β-Catenin
DAPI

f)

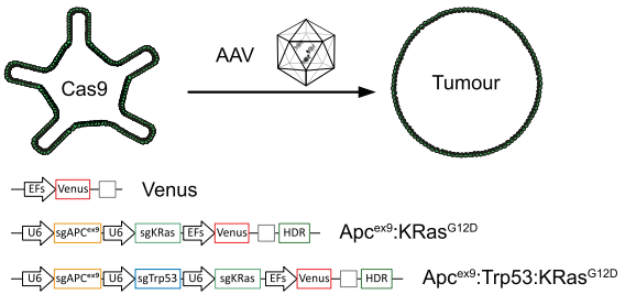
Cas9
AAV
Tumour
Venus
Apcex9:KRasG12D
Apcex9:Trp53:KRasG12D

g)

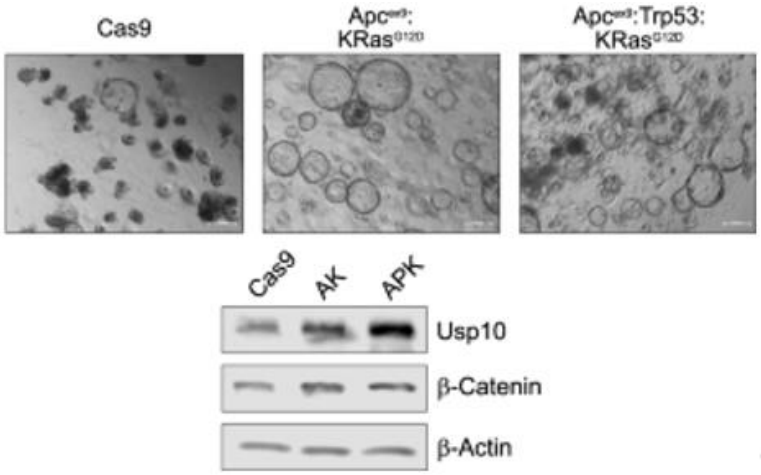

h)

Figure 2. Murine intestinal cancer models reveal early USP10 upregulation in CRC development

a Illustration of the murine small intestine and colon. Villi were mechanically removed, and crypts from the small intestine and colon were isolated using EDTA. Samples from two mice were analyzed for endogenous USP10, β-Catenin, and Krt20 levels. β-Actin served as a loading control (n = 2).

b Immunofluorescence of WT intestinal crypts showing USP10 (green) and cell type-specific markers. Upper panel: Lysozyme (magenta) marks Paneth cells; lower panel: Cd44 (magenta) identifies stem cells. DAPI (blue) marks nuclei. White lines indicate regions quantified for fluorescence intensity, with corresponding histograms.

c Schematic of acute CRC induction in CD1 mice via colorectal delivery of lentiviral sgRNA targeting Apc exon 10 (Apcex10) alongside constitutive SpCas9 expression (pLenti-CRISPR-V2). pr.i. – pre-infection.

d H&E staining of tumors 12 weeks post-viral delivery. Insets show non-transformed adjacent tissue versus primary tumor following Apc editing.

e Immunofluorescence images of USP10 (green) and β-Catenin (red) in crypts from panels a and b. DAPI (blue) marks nuclei. Insets: untransformed (1) vs. transformed (2) regions. Quantification performed with QuPath; individual cells shown as dots. Mann–Whitney test applied. ***$p < 0.001$.

f High-magnification immunofluorescence of USP10 (green) and β-Catenin (red) in CRISPR-infected intestines. DAPI marks nuclei (blue).

g Schematic of CRISPR-modified murine CRC models using AAV to deliver sgRNAs and HDR templates targeting APC (exon 9), Trp53, or introducing KrasG12D.

h Brightfield images of murine intestinal organoids: wild-type (Cas9), Apc:KrasG12D (AK), or Apc:Trp53:KrasG12D (APK). Immunoblots show USP10 and β-Catenin expression. β-Actin as control.

Motivated by USP10 expression in normal intestinal crypts, we examined whether its levels rise during tumor initiation. Histological analysis of tumors from mice, generated either by acute CRISPR-mediated Apc truncation (APCex10) or via heterozygous Apc loss in Apcmin/+ animals, revealed strong upregulation of USP10 protein in tumor tissues along with elevated β-Catenin, relative to non-transformed intestinal epithelium (**Figures 2c–f**).

To determine whether specific genetic alterations drive USP10 upregulation, we employed wild-type organoids (Cas9) and generated Apc:KrasG12D (AK) and Apc:Trp53:KrasG12D (APK) organoids via CRISPR (**Figures 2g**, **h and 2g**). Loss of Apc caused morphological changes and reduced reliance on WNT ligands in culture. KrasG12D mutation enhanced Erk1/2 signaling and bypassed the need for EGF supplementation [32]. In transformed organoids, USP10 and β-Catenin were significantly increased compared to parental controls (**Figure 2h**).

These results indicate that USP10 upregulation is an early CRC event, occurring independently of the number or complexity of oncogenic driver mutations, and coincides with higher β-Catenin abundance.

Truncated APC enables direct interaction between USP10 and β-Catenin in CRC

We hypothesized that USP10 forms a complex with β-Catenin in CRC, dependent on mutations in either β-Catenin or APC. Co-immunoprecipitation experiments in HCT116 (CTNNB1mut/APCwt) and HT-29 (CTNNB1wt/APCtruncated) cells revealed that USP10 and β-Catenin do not associate in HCT116, but co-precipitate in HT-29 cells (**Figures 3a and 3b)**, suggesting that APC truncation facilitates this interaction.

To validate this, a panel of human CRC cell lines (LS174T, DLD-1, SW480, SW620, Caco-2, Colo320) with distinct APC truncations was analyzed (**Figures 3b and c).** USP10 and β-Catenin co-immunoprecipitation was detected only in Colo320, indicating that proximal APC truncations are required, while distal truncations (DLD-1, Caco-2, SW480/SW620) did not support the interaction (**Figures 3b and c**).

APC truncation may have clinical implications: survival analysis of CRC patients stratified by APC mutation location (within first 1000 amino acids, distal, or point mutations) revealed a trend toward shorter survival in carriers of short APC variants (**Figure 3a**).

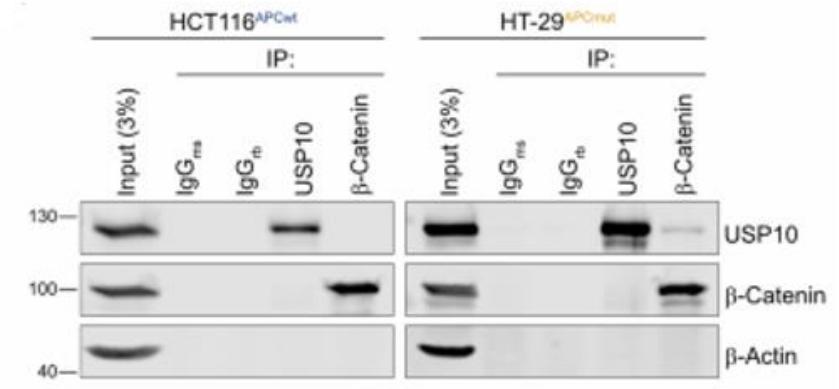

a)

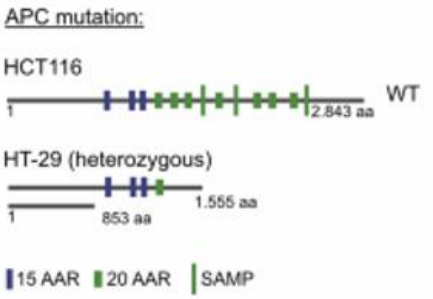

b)

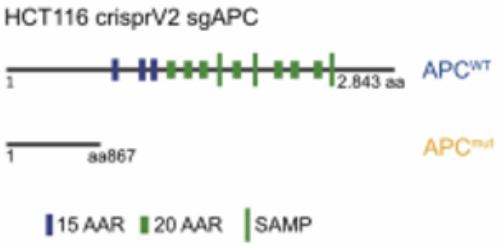

c)

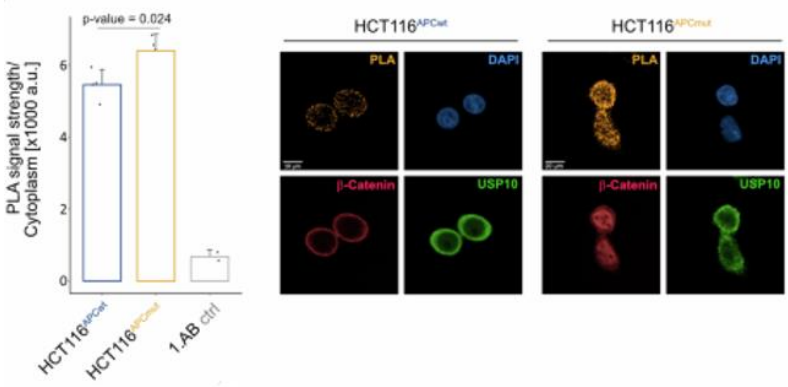

d)

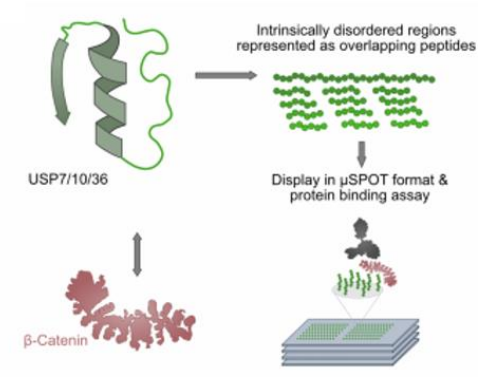

e)

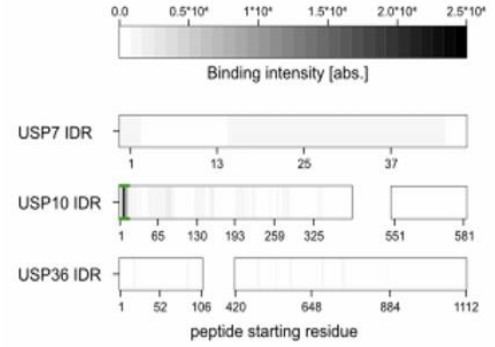

f)

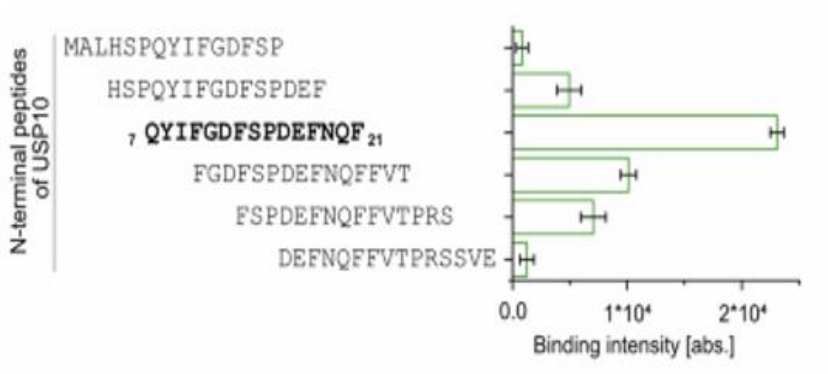

g)

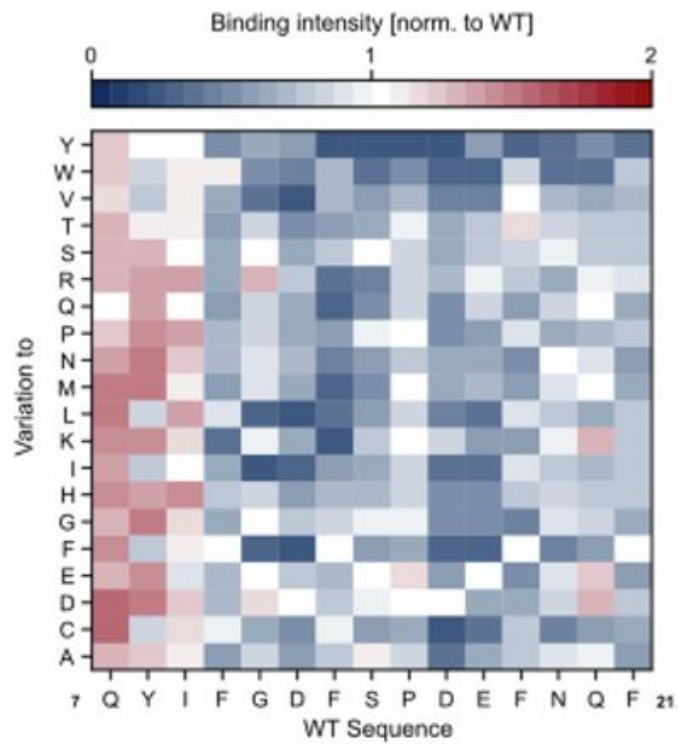

h)

Figure 3. APC truncation permits a novel interaction between USP10 and β-Catenin in CRC

a Representative inputs and endogenous co-immunoprecipitation of USP10 and β-Catenin in human CRC cell lines: HCT116 (APC wild-type) and HT-29 (APC truncated). IgG was used as a specificity control, and β-Actin served as a loading control. Inputs correspond to 3% of the total protein. n = 3.

b Diagram summarizing reported truncating mutations within APC in HCT116 and HT-29. Dark blue boxes: 15 AAR repeats; small green boxes: 20 AAR repeats; large green boxes: SAMP domains. 15- and 20-AAR = β-Catenin binding repeats; SAMP = Axin interaction sites. Adapted from www.uniprot.org.

c Model of acute APC truncation at residue 867 in HCT116 cells using CRISPR.

d Quantification of proximity ligation assays (PLA) between USP10 and β-Catenin in HCT116 cells, either APCwt or CRISPR-truncated APC867 (APCmut). Data derived from >750 cells across two independent experiments. Mann–Whitney U test for statistics. Representative immunofluorescence images show USP10 (green), β-Catenin (red), and PLA signal (mustard). DAPI (blue) marks nuclei. n = 2.

e Schematic of the μSPOT peptide-binding assay. Intrinsically disordered regions (IDRs) of USP7, USP10, and USP36 were defined by <50 pLDDT in AlphaFold2 predictions and represented as overlapping 15-mer peptides (overlap of 11–12 amino acids). Recombinant β-Catenin was incubated on the μSPOT slides, and binding was detected by chemiluminescent immunostaining.

f Heatmap of β-Catenin binding to IDRs of USP7, USP10, and USP36. Gaps indicate structured domains. Highest affinity region within USP10 (residues 7–21, N-terminal) highlighted.

g Bar graph showing binding intensity of USP10 N-terminal peptide 7QYIFGDFSPDEFNQF21 to recombinant β-Catenin. Mean ± SD; n = 3.

h Positional scan of USP10 residues 7–21. Each amino acid was substituted with all other proteogenic residues, and relative β-Catenin binding intensity was measured. Certain substitutions dramatically reduced binding, indicating direct interaction of specific side chains. Mean ± SD; n = 3.

Based on HT-29 and Colo320 genetics, we concluded that the 15- and 20-AAR domains of APC are necessary to compete with USP10 for β-Catenin binding. Therefore, the novel USP10–β-Catenin interaction appears dependent on loss of these AAR repeats. PLA in HCT116 cells with or without CRISPR-induced APC truncation confirmed that intact APC competes with USP10 for β-Catenin binding (**Figures 3c and 3d**).

To map the USP10 binding site, we performed a μSPOT protein binding assay [33]. IDRs from USP10, USP7 (a known β-Catenin binder [13]), and USP36 were probed with recombinant β-Catenin (**Figure 3e).** USP10 residues 7–21 (7QYIFGDFSPDEFNQF21) mediated strong direct binding (**Figures 3f–h**). Competitive assays revealed that this USP10 peptide reduced β-Catenin binding to AXIN1 and APC, suggesting high-affinity binding of β-Catenin to USP10 and TCF4 (**Figures 3d and 3e**). Co-immunoprecipitation in HT-29 cells transduced with wild-type USP10 or a Δ7–21 mutant showed diminished β-Catenin interaction for the mutant (**Figure 3f**). AlphaFold2 Multimer modeling (AF2M) confirmed that the same USP10 residues engage β-Catenin, overlapping with APC and AXIN1 binding regions (**Figure 3g and 3h**).

Overall, we identified a direct USP10–β-Catenin interaction and demonstrated that APC and USP10 compete for the same β-Catenin binding site, providing a molecular basis for the β-Catenin stabilization observed in APC-truncated CRC.

Acute USP10 depletion in D. melanogaster intestinal stem cells rescues hyperplasia and lethality in the ApcQ8/Q8 model

Given the conservation of USP10 and Wnt signaling across species, we investigated its role in intestinal homeostasis using D. melanogaster [34] (aa similarity: 379/821, 46%; identity: 254/821, 30%; gaps: 185/821, 22%; https://www.flyrnai.org/cgi-bin/DRSC_prot_align.pl?geneid1=38103&geneid2=9100; **Figures 4**).

We first tested shRNA-mediated knockdown of dUSP10 in intestinal progenitors, marked by GFP under the escargot promoter (esg::GAL4 > GFP). Armadillo (the fly β-Catenin ortholog) immunofluorescence in intestinal stem cells (ISCs) revealed that dUSP10 knockdown significantly reduced ISC numbers compared with LacZ control shRNA (**Figures 4a and 4b**).

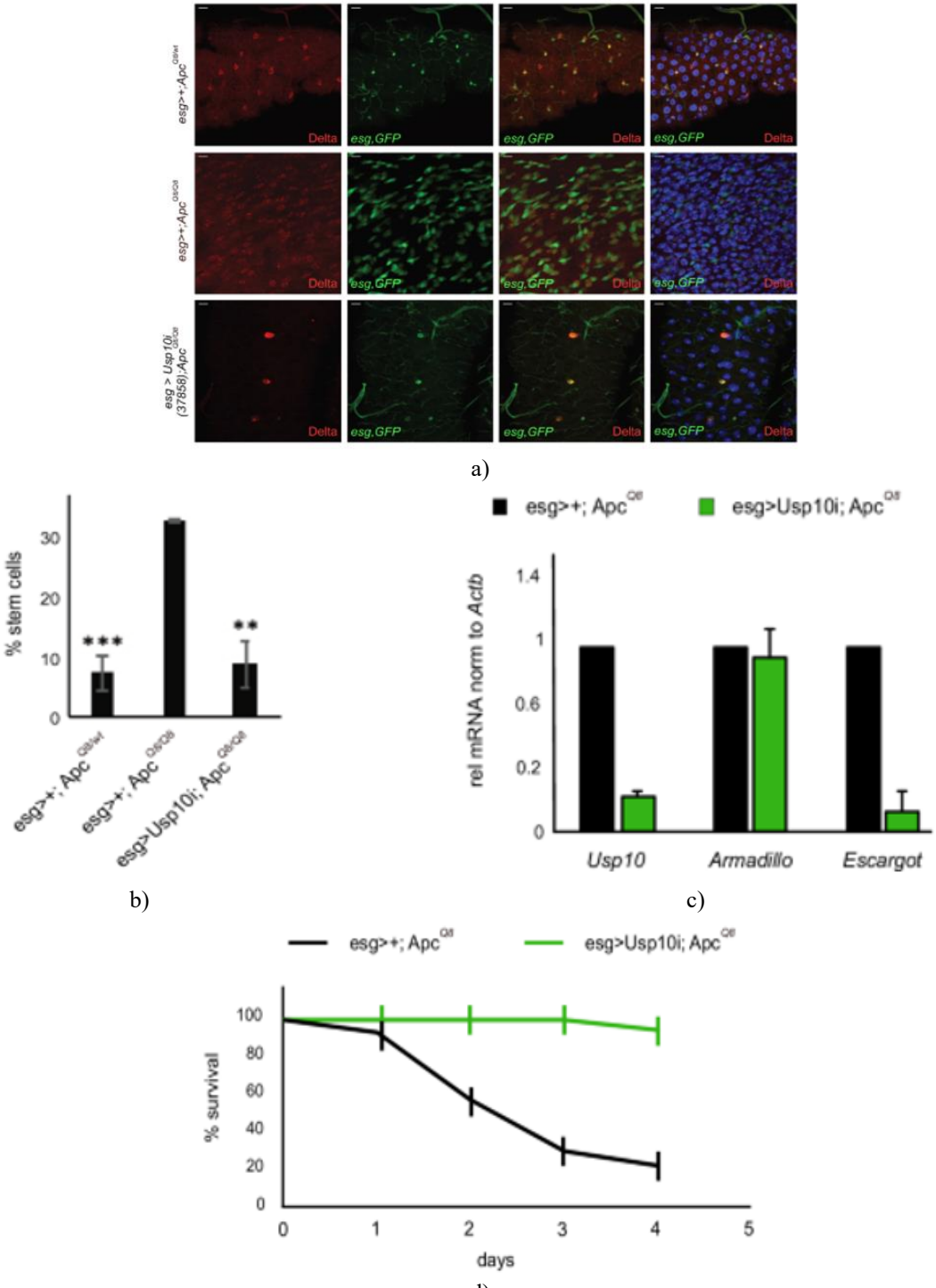

Figure 4. Acute USP10 depletion in D. melanogaster intestinal stem cells rescues hyperplasia and lethality in ApcQ8/Q8 mutants

a Representative immunofluorescence of fly midguts. Heterozygous ApcQ8/+ animals exhibit midguts largely indistinguishable from wild-type (not shown). In contrast, homozygous ApcQ8 mutants display excessive proliferation of intestinal stem cells (ISCs) marked by Delta (red). RNAi-mediated USP10 knockdown (UAS-IR) alleviates this progenitor hyperproliferation phenotype in ApcQ8 homozygotes.

b Quantification of total ISC numbers across the three conditions. Statistical significance relative to "esg > +; ApcQ8" was calculated using one-way ANOVA. **p < 0.005; ***p < 0.001.
c qRT-PCR analysis of USP10, armadillo, and escargot transcripts from midguts of ApcQ8 and ApcQ8 USP10KD flies. Expression normalized to Actb; error bars represent SD of three biological replicates.
d Kaplan–Meier survival curves of adult flies: ApcQ8 n = 24, ApcQ8:esg-USP10i n = 17.

To assess genetic interaction between truncated APC and USP10, we used the ApcQ8 hyperplasia model [35]. The ApcQ8 allele carries a premature stop codon, producing truncated APC lacking β-Catenin binding domains. Immunofluorescence revealed that heterozygous ApcQ8 midguts maintain near-normal tissue architecture, similar to wild-type. In contrast, ApcQ8/Q8 homozygotes exhibit disorganized midguts densely populated with escargot-positive progenitors, many expressing the ISC marker Delta (**Figures 4a and 4b**). Transcriptional profiling revealed elevated dUSP10 mRNA in ApcQ8/Q8 midguts (**Figure 4e**), mirroring patterns observed in human and murine CRC models. Knockdown of dUSP10 suppressed progenitor expansion, restoring midgut morphology to a more normal state (**Figures 4a and 4b**). Analysis of isolated midguts confirmed a significant reduction of USP10 transcripts and decreased escargot expression in USP10i;ApcQ8/Q8 flies (**Figures 4c and 4e**).

We next evaluated the effect of dUSP10 depletion on fly survival. Heterozygous ApcQ8/wt flies showed normal longevity, while ApcQ8/Q8 homozygotes exhibited temperature-sensitive lethality (**Figures 4d and 4f**). Expression of shRNA against dUSP10 in intestinal progenitors (USP10i;ApcQ8/Q8) rescued survival, likely by mitigating hyperplasia and tissue disorganization caused by APC truncation (**Figure 4d**).

These data indicate an epistatic genetic interaction between USP10 and truncated APC that is essential for ectopic stem cell proliferation.

USP10 regulates WNT signaling and stemness-associated genes via β-Catenin stabilization

To explore USP10 function in APC-truncated CRC, we deleted endogenous USP10 by targeting exons 2 and 10 in HT-29 and HCT116 cells, respectively (**Figure 5a**). USP10 depletion in HT-29 markedly reduced β-Catenin levels and the CRC/WNT target LGR5 (**Figures 5a and 5b)**. Loss of USP10 enhanced β-Catenin ubiquitylation (**Figure 5c**) and accelerated its degradation (**Figure 5d**, quantified in 5e). In HCT116, which retains wild-type APC, USP10 deletion did not affect β-Catenin abundance or ubiquitylation, confirming that USP10's regulatory effect depends on APC truncation.

Interestingly, CRISPR-mediated USP10 knockout in HT-29 reduced β-Catenin levels but prevented long-term propagation, as edited cells were outcompeted by wild-type cells within the population, consistent with previous reports of cell lethality upon USP10 loss [36]. To bypass this issue, an inducible shRNA system was used to acutely deplete USP10 in HT-29 (two independent shRNAs, **Figure**. **5f**). USP10 knockdown led to a pronounced reduction in proliferation compared with control cells (**Figure 5g**).

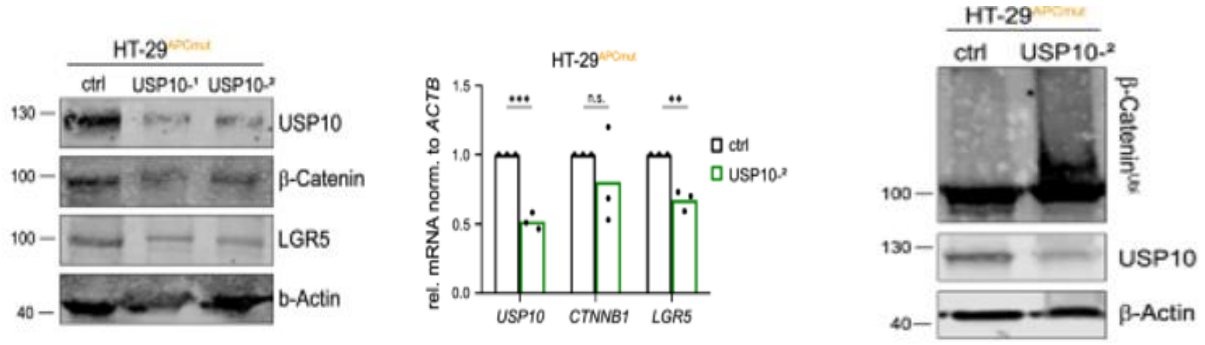

a) b) c)

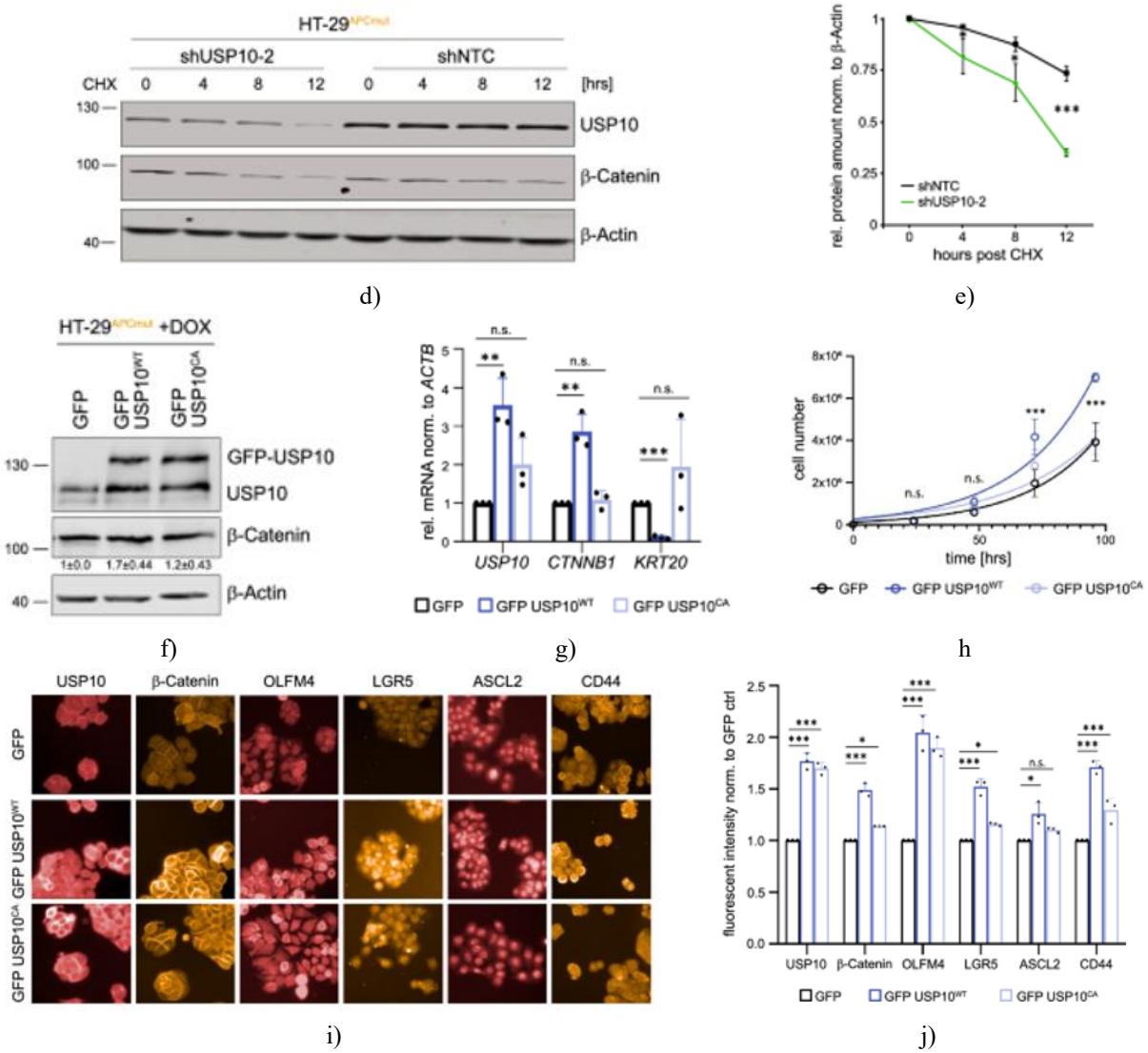

Figure 5. USP10 controls WNT signaling and stemness-related genes by stabilizing β-Catenin

a Immunoblot analysis of endogenous USP10, β-Catenin, and LGR5 in APC-mutant HT-29 cells following CRISPR-mediated USP10 deletion. Two independent CRISPR pools (USP10−1, USP10−2) and non-targeting control (ctrl) are shown. β-Actin served as a loading control. n = 3.

b qRT-PCR of USP10, CTNNB1, and LGR5 in USP10−2 HT-29 cells compared to ctrl. Error bars indicate SD from three independent experiments; significance calculated by Student's t-test. **p < 0.005; ***p < 0.001; n.s. non-significant.

c TUBE assay for endogenous poly-ubiquitylated proteins, followed by immunoblot for β-Catenin in USP10−2 HT-29 cells. Endogenous USP10 immunoblot shown; β-Actin as loading control. n = 2.

d Cycloheximide (CHX, 100 µg/ml) chase assay in shNTC or shUSP10-2 HT-29 cells over the indicated times. Representative immunoblot for USP10 and β-Catenin; β-Actin loading control. n = 3.

e Quantification of β-Catenin levels normalized to β-Actin from d. Significance assessed by Student's t-test. n = 3; *p < 0.05; ***p < 0.001.

f Immunoblot of HT-29 cells with DOX-inducible expression of GFP control, wild-type GFP-USP10 (GFP USP10WT), or catalytic inactive GFP-USP10 mutant (GFP USP10CA). β-Actin loading control. n = 3.

g qRT-PCR for USP10, CTNNB1, and KRT20 in HT-29 overexpressing USP10 variants. Error bars indicate SD of n = 3 independent experiments; significance by

Student's t-test. **p < 0.005; ***p < 0.001; n.s. non-significant.

h Growth curves of HT-29 cells expressing GFP USP10WT or GFP USP10CA versus GFP control. n = 3; one-way ANOVA. ***p < 0.001; n.s. non-significant.

i Representative immunofluorescence of USP10WT, USP10CA, and GFP control HT-29 cells.

j Quantification of i; mean fluorescence intensity normalized to GFP control. n = 3; unpaired t-test. *p < 0.05; ***p < 0.001; n.s. non-significant.

Analysis of HT-29 proteomes after 24 h siRNA-mediated USP10 knockdown revealed downregulation of stem cell niche proteins, including TCF4 (TCF7L2), TNFRSF21, NOTCH2, LGR4, CD44, and the WNT target MYC (**Figures 5h and 5i**).

For gain-of-function experiments, wild-type USP10 (USP10WT) or catalytic inactive USP10 (USP10CA) were conditionally overexpressed in HT-29. USP10WT increased β-Catenin protein and mRNA, whereas USP10CA failed to do so (**Figures 5f and 5g**). Overexpression of USP10WT enhanced proliferation compared to controls (**Figure 5h**). Immunofluorescence of HT-29 expressing USP10WT demonstrated upregulation of stem niche markers β-Catenin, OLFM4, LGR5, ASCL2, and CD44, which was absent in USP10CA cells (**Figures 5i and 5j**).

Collectively, these data indicate that USP10 stabilizes β-Catenin in an APC-truncation dependent manner, promoting WNT signaling, stemness signatures, and CRC cell growth.

USP10 is essential for CRC cell identity, stemness, and tumorigenesis

To determine USP10 dependency in patient-relevant models, we used patient-derived organoids (**Figure 6a**). Line P6T carries a truncating APC mutation (R876*) along with a longer APC variant (P1420fs), analogous to HT-29. Three weeks post-infection with either control shRNA (shNTC) or USP10-targeting shRNA, organoids were analyzed (**Figures 6b–h**). USP10 depletion significantly reduced organoid size and number (**Figures**. **6c and 6d**). Transcriptomic profiling revealed that USP10 regulates WNT signaling, stem cell maintenance, and differentiation (**Figures 6f and 6g**). Stem cell-related genes LGR5, LEF1, AXIN2, and LRIG1 decreased upon USP10 loss, while differentiation markers MUC2 and KRT20 increased. Loss of USP10 also upregulated stress response gene sets, including UPR and ROS signaling (**Figure**. **6h**).

These results align with observations in HT-29 cells and demonstrate that USP10 sustains a pro-tumorigenic, stem cell-like state, required for CRC growth.

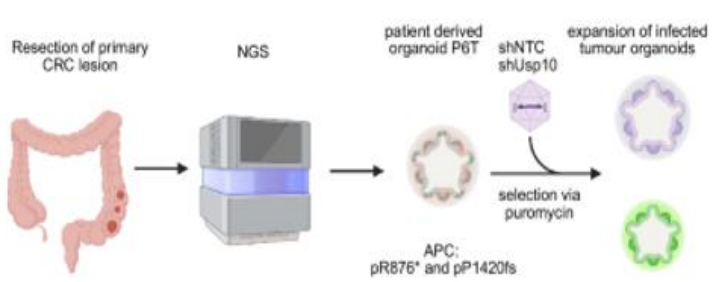

a)

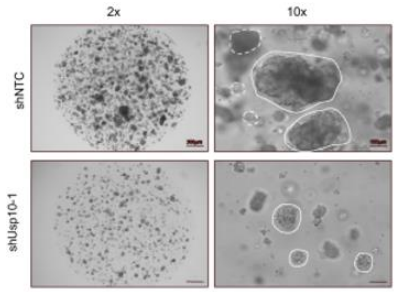

b)

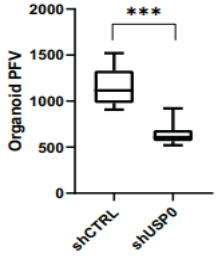

c)

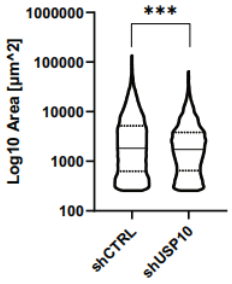

d)

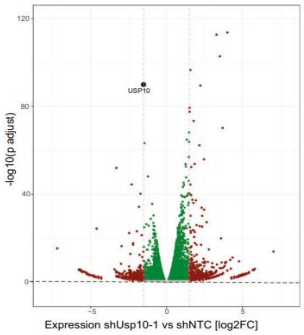

e)

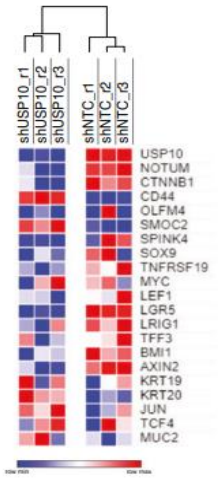
shUSP10_r1
shUSP10_r2
shUSP10_r3
shNTC_r1
shNTC_r2
shNTC_r3
USP10
NOTUM
CTNNB1
CD44
OLFM4
SMOC2
SPINK4
SOX9
TNFRSF19
MYC
LEF1
LGR5
LRIG1
TFF3
BMI1
AXIN2
KRT19
KRT20
JUN
TCF4
MUC2

f)

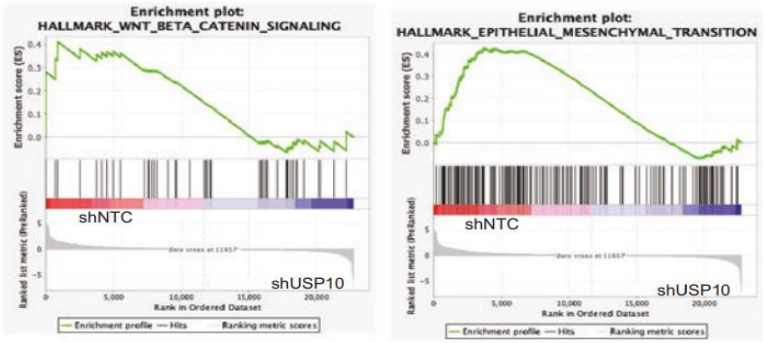
Enrichment plot:
HALLMARK_WNT_BETA_CATENIN_SIGNALING
shNTC
shUSP10
Enrichment plot:
HALLMARK_EPITHELIAL_MESENCHYMAL_TRANSITION
shNTC
shUSP10

g)

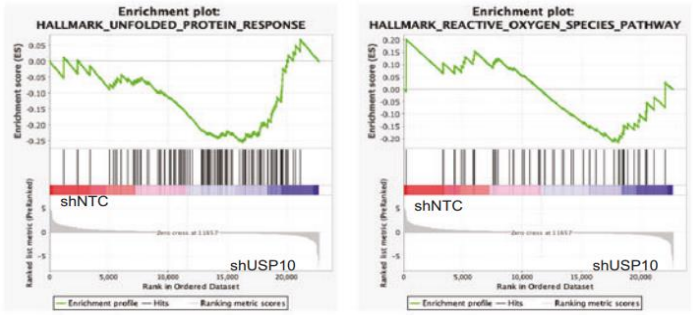
Enrichment plot:
HALLMARK_UNFOLDED_PROTEIN_RESPONSE
shNTC
shUSP10
Enrichment plot:
HALLMARK_REACTIVE_OXYGEN_SPECIES_PATHWAY
shNTC
shUSP10

h)

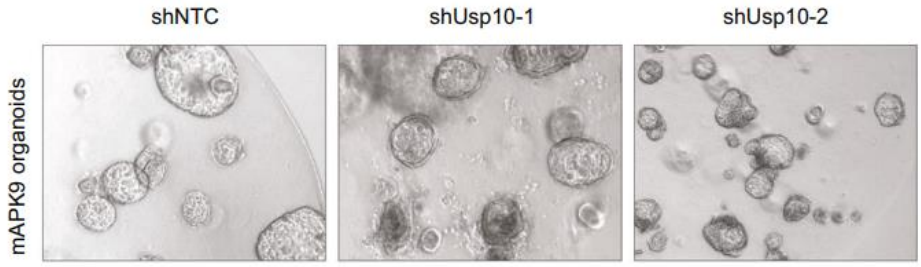
shNTC
shUsp10-1
shUsp10-2
mAPK9 organoids

i)

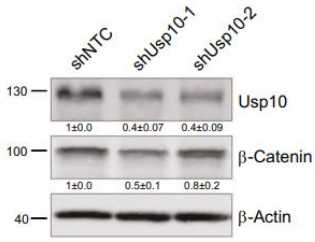
shNTC
shUsp10-1
shUsp10-2
130
Usp10
1±0.0
0.4±0.07
0.4±0.09
100
β-Catenin
1±0.0
0.5±0.1
0.8±0.2
40
β-Actin

j)

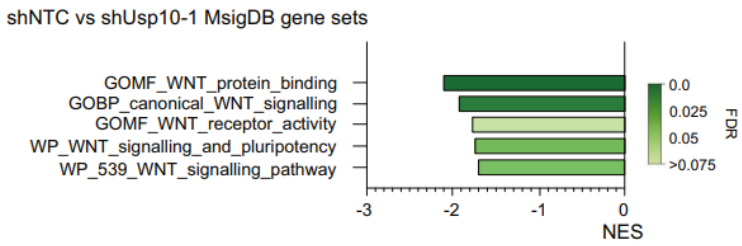
shNTC vs shUsp10-1 MsigDB gene sets
GOMF_WNT_protein_binding
GOBP_canonical_WNT_signalling
GOMF_WNT_receptor_activity
WP_WNT_signalling_and_pluripotency
WP_539_WNT_signalling_pathway
-3
-2
-1
0
NES
0.0
0.025
0.05
>0.075
FDR

k)

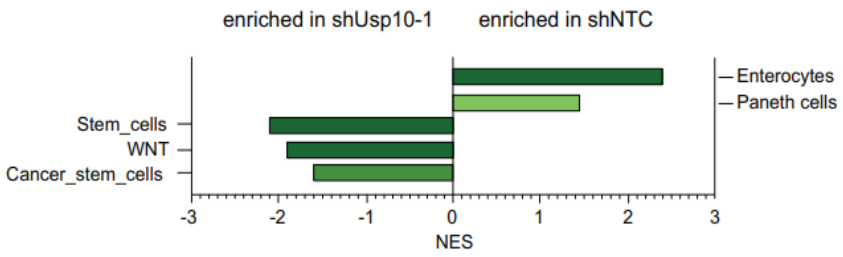

l)

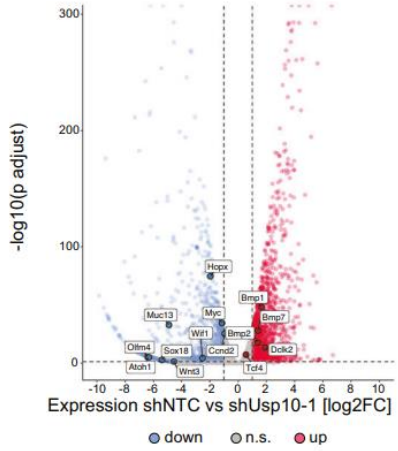

m)

Figure 6. USP10 is necessary for CRC cell identity, stemness, and tumorigenic growth

a Workflow schematic illustrating the isolation, characterization, and USP10 knockdown in patient-derived CRC organoid line P6T (Oncode Organoid Bank).

b Brightfield images of stably transformed human P6T organoids infected with either USP10-targeting shRNA or a non-targeting control. n = 10 fields of view. Individual intact organoids are highlighted.

c Quantification of organoid number per field one week post-infection with control (shNTC) or shUSP10. Statistical significance was determined using an unpaired t-test; $p < 0.0001$. Images quantified via QuPath v0.4.2 and ImageJ (FIJI). Boxplots generated in GraphPad Prism8; center line represents median, box limits first and third quartiles, whiskers 1.5× IQR. Mann–Whitney U test: ***$p < 0.0001$.

d Quantification of relative organoid size per field one week post-infection with shNTC or shUSP10. n = 10 fields; statistics as in c. Violin plots generated in GraphPad Prism8; Mann–Whitney U test: ***$p < 0.0001$.

e Volcano plot depicting differential gene expression in P6T organoids following USP10 knockdown compared to shNTC control. Significantly altered genes in red; USP10 highlighted. n = 3.

f Heatmaps showing expression of WNT pathway, differentiation, and NOTUM-associated genes in shNTC versus shUSP10 P6T organoids. n = 3.

g, h GSEA of P6T organoids expressing shUSP10 or shNTC. Enrichment plots show WNT signaling, EMT, UPR, and ROS pathways.

i Brightfield images of murine APK9 organoids (Aex9PKG12D) expressing either shNTC or two independent shRNAs targeting USP10.

j Immunoblot for USP10 and β-Catenin in shRNA-treated APK9 organoids. β-Actin served as loading control; quantification n = 3.

k, l GSEA showing MsigDB gene sets (k) and intestine-specific gene sets (l) deregulated in shUSP10-1 versus shNTC APK9 organoids.

m Volcano plot showing differential expression in APK9 organoids following USP10 knockdown. Up- and downregulated genes highlighted in red and blue, respectively; genes of interest labeled.

To test conservation in murine models, intestinal APK9 organoids were transduced with AAV encoding

shUSP10 or control shRNA (**Figures 6i–m**,). USP10 depletion was confirmed by immunoblot (**Figure 6j**). Transcriptomic analysis revealed that USP10 is critical for WNT signaling maintenance; loss of USP10 markedly reduced β-Catenin levels and downstream targets Myc and Ccnd2 (**Figures 6k–m**,). Overall, USP10 knockdown decreased stemness-associated signatures and increased differentiation gene expression (**Figures 6k and** 6**l**).

These data indicate that USP10 governs differentiation and contributes to intestinal cancer cell identity, promoting cancer stemness and proliferation through β-Catenin.

Loss of USP10 counteracts competitor signaling and restores normal stem cell niches

Recent studies demonstrated that CRC cells eliminate adjacent non-transformed intestinal stem cells via Apc-dependent NOTUM signaling, a phenomenon termed the "super-competitor" phenotype, which is essential for tumor growth [28, 29, 37]. Given USP10's effect on WNT signaling and β-Catenin, we tested whether USP10 is necessary for this phenotype. Wild-type organoids were cultured in conditioned media from either APKshNTC or APKshUSP10 organoids (**Figures 7a and 7b**). Exposure to APKshNTC media led to rapid loss of wild-type organoids, whereas media from USP10-depleted organoids allowed prolonged survival (**Figures**. **7a and 7b**).

Transcriptomic analysis of APKshUSP10-2 organoids showed downregulation of Notum and super-competitor-associated genes (Dkk2, Dkk3, Wif1) upon USP10 loss (**Figure**. **7b**), consistent with NOTUM downregulation in patient-derived CRC organoids after USP10 silencing (**Figure 6f**).

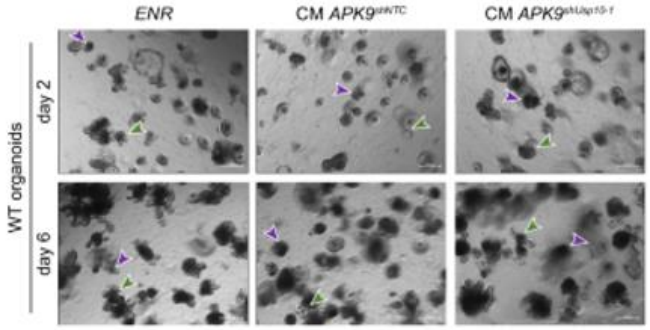

a)

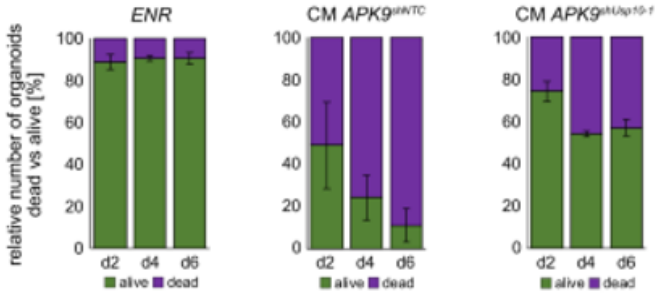

b)

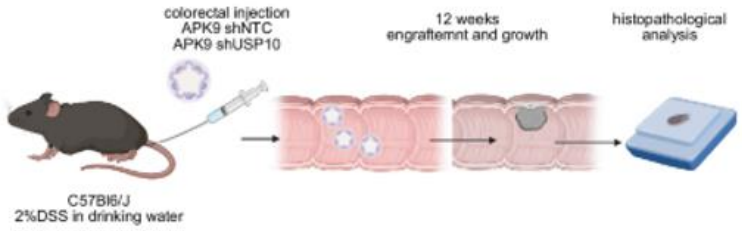

c)

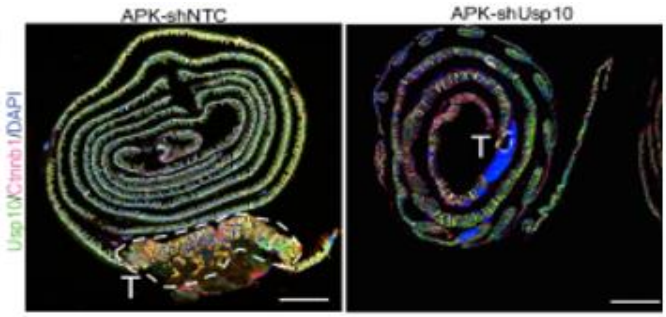

d)

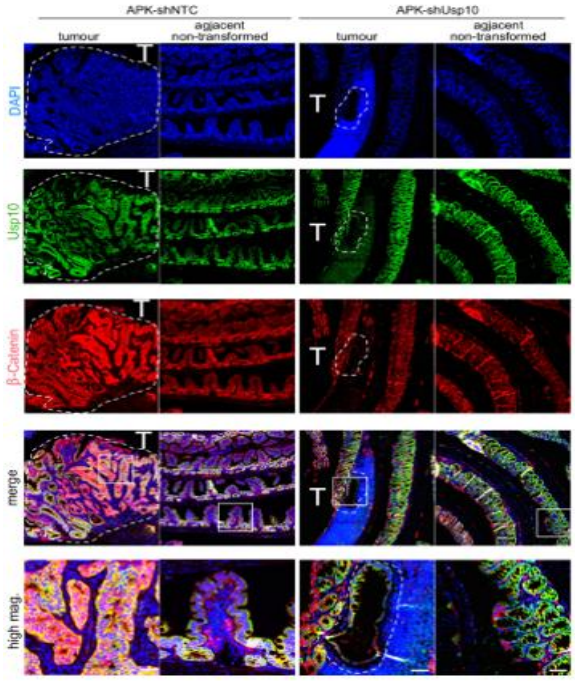

e)

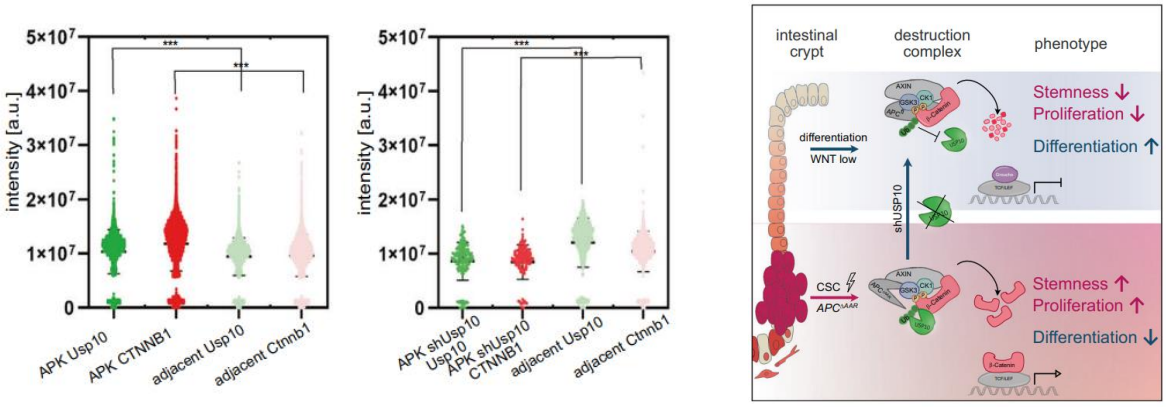

f) g)

Figure 7. Silencing USP10 counteracts super-competitor signaling and reinstates normal stem cell niches

a Brightfield images of wild-type (WT) intestinal organoids cultured in ENR medium, or in conditioned media (CM) derived from APKshNTC and APKshUSP10-1 organoids, supplemented with EGF, Noggin, and R-spondin, over 6 days. Dead organoids are

indicated with purple arrows, viable ones with green arrows. E – EGF, N – Noggin, R – R-spondin. n = 3.

b Quantitative analysis of organoid viability per condition. Bars represent the percentage of live versus dead organoids. Error bars correspond to standard deviations across three independent experiments.

c Diagram of the in vivo transplantation setup: APK organoids expressing either shNTC or shUSP10 were introduced into immunocompetent C57Bl6/J mice (adapted from [38-40]).

d Merged immunofluorescence of transplanted murine intestines showing endogenous USP10 (green) and β-Catenin (red). Tumour regions originating from engrafted organoids are circled. DAPI marks nuclei. Scale bar: 1 mm.

e Close-up images of individual tumors and adjacent non-tumorous areas. USP10 (green) and β-Catenin (red) are visualized. Tumour boundaries are outlined. Scale bars: overview 200 µm; inset 50 µm.

f Relative fluorescence quantification (arbitrary units, a.u.) of USP10 and β-Catenin in shNTC vs. shUSP10 conditions. Statistical significance determined by unpaired t-test; ***$p < 0.0001$. Analyses performed using QuPath v0.4.2; boxplots generated in GraphPad Prism8 with single-cell data points.

g Model: In CRC with APC truncation, deletion of AAR domains enables USP10 to form a novel interaction with β-Catenin. This stabilizes β-Catenin, driving target gene transcription, stem-like properties, and proliferation while suppressing differentiation. Suppression of USP10 by shRNA or CRISPR/Cas9 reverses these effects, reducing stemness and increasing differentiation.

To test the functional impact of USP10 in vivo, APK9 organoids expressing shNTC or shUSP10 were transplanted into immunocompetent C57Bl6/J mice (**Figure 7c**). At 24 weeks post-transplant, tissue analysis revealed that shNTC organoids formed large tumors, consistent with prior reports [38, 39, 41]. USP10 knockdown organoids were still engrafted but generated smaller lesions (**Figures 7d–f**). Tumors derived from shNTC organoids had high levels of USP10 and β-Catenin, while USP10-depleted tumors exhibited reduced β-Catenin (**Figures 7e and 7f**). Morphologically, shNTC tumors resembled invasive carcinoma, whereas shUSP10 tumors had more mucus-producing cells (**Figure**. **7e**, star).

These findings indicate that USP10 is critical for maintaining WNT-driven stemness, β-Catenin stabilization, and tumor progression. Its inhibition diminishes the super-competitor phenotype, promotes differentiation, and limits tumor growth, identifying USP10 as a key vulnerability in CRC during both tumor initiation and expansion.

Colorectal cancer development is largely driven by dysregulated WNT signalling, which leads to persistent activation of the proto-oncogene β-Catenin and continuous transcription of its downstream targets [11]. This is primarily initiated through loss-of-function mutations in the tumor suppressor APC, with approximately 80% of CRC patients carrying such alterations [4, 26]. Notably, the position of truncating mutations within APC determines which functional domains remain [7]. Recent evidence suggests that tumor progression, loss-of-heterozygosity, and aberrant WNT signalling are influenced by the residual length of APC [42]. Moreover, APC truncations are essential for establishing a super-competitor cell phenotype, a process that facilitates CRC initiation [28, 29, 33]. Despite progress in understanding the genetic drivers of CRC, defining the molecular mechanisms underlying these events and identifying viable therapeutic targets remains a significant challenge [43].

One potential strategy is to target elevated oncoprotein stability, particularly through modulation of the Ubiquitin Proteasome System (UPS) [44]. Even in the absence of functional APC or when β-Catenin carries degron motif mutations, the WNT effector remains subject to ubiquitylation in CRC cell lines [7, 9]. Several E3 ligases have been shown to regulate β-Catenin stability and activity through ubiquitylation [16–20], suggesting that its protein abundance could be therapeutically manipulated by targeting stabilizing enzymes. In this context, deubiquitylases (DUBs) represent an attractive druggable class, as they counteract substrate ubiquitylation and contribute to protein stabilization and activation [45].

In our study, we explored whether DUBs could modulate β-Catenin levels in CRC driven by APC loss. An unbiased screen revealed USP10 as a factor that increases β-Catenin abundance. USP10 has previously been implicated in regulating TP53 stability [46, 47], autophagy [48, 49], DNA damage responses [50, 51], and metabolic pathways [51, 52]—all critical for tumor cell survival [53]. Analysis of patient datasets and local CRC samples demonstrated frequent upregulation of USP10, often in parallel with β-Catenin expression. Notably, USP10 only interacted with β-Catenin when APC truncation removed the AAR domains, a finding

confirmed by CRISPR-mediated APC truncation in otherwise wild-type CRC lines. Microarray-based peptide binding assays mapped residues 7–21 of USP10's unstructured N-terminal region as the direct β-Catenin binding site. Structural modeling indicated that this site overlaps with the APC binding interface, providing a molecular explanation for the requirement of APC truncation for USP10 interaction. This overlap may also explain how APC mutations indirectly modulate β-Catenin protein levels without changing its ubiquitylation status. Collectively, our findings extend the understanding of WNT signalling in CRC and suggest a stratification of patients based on USP10 dependency, presenting APC not only as a diagnostic marker but also as a potential therapeutic vulnerability. Additionally, our study highlights a direct USP10-β-Catenin interaction, confirming their role in regulating tumor-intrinsic processes. Interestingly, in NSCLC, USP10 has been shown to stabilize HDAC7, which in turn affects β-Catenin levels [54], demonstrating tissue- and context-specific mechanisms.

An alternative mechanism of WNT regulation by USP10 was recently reported in zebrafish, where USP10 promoted β-Catenin degradation by stabilizing AXIN1 [55]. This emphasizes the potential substrate and context specificity of USP10, consistent with observations for other UPS members such as USP28 [56–58]. In cancer, USP10 exhibits dual roles as a proto-oncogene or tumor suppressor, sometimes even within the same tumor type, as shown in NSCLC [54, 59]. The underlying reasons for these opposing functions remain unclear, highlighting the need for careful functional dissection to define USP10's therapeutic potential.

In APC-truncated CRC, USP10 modulates β-Catenin ubiquitylation, with broad consequences for tumor biology. Alterations in USP10 levels affected the expression of genes associated with proliferation, stemness, and disease progression. USP10 supports the cellular identity of CRC cells, as its loss shifts transcriptional profiles toward a differentiated, non-transformed state. Beyond intrinsic WNT-mediated pathways, USP10 depletion reduced the cell death of non-transformed cells exposed to conditioned medium from tumor organoids, counteracting the super-competitor phenotype [28, 29, 37]. Importantly, these effects were dependent on USP10's catalytic activity; overexpression of a catalytically inactive form failed to influence β-Catenin abundance or cell proliferation, highlighting the catalytic site as a promising therapeutic target [60].

The alterations in gene expression seen in USP10 shRNA-treated CRC cell lines and organoids are a direct outcome of diminished β-Catenin protein levels. These regulatory effects appear to be highly conserved across species. Using D. melanogaster models of intestinal hyperproliferation, we demonstrated that silencing USP10 in the intestinal stem cell compartment mitigated the pathological phenotype caused by homozygous APC loss (APCQ8/Q8) [34]. Comparable results were observed in organoid transplantation experiments. These findings align with prior studies showing that inhibiting NOTUM in both established and transplanted CRC tumors can restrain tumor progression [41]. Accordingly, pharmacological inhibition of USP10 with small-molecule compounds [61] could offer additional therapeutic strategies for CRC.

By combining analyses of human CRC patient material, cultured colorectal cancer cell lines, genetically modified murine organoids, and D. melanogaster as a model for intestinal WNT dysregulation, we identified a previously uncharacterized protein-protein interaction essential for CRC cell survival. Collectively, these experiments provide strong in vitro and in vivo evidence that USP10 drives CRC progression and represents a potential therapeutic target, particularly in patients with APC truncations.

Ethics approval and consent to participate

All animal studies involving CRISPR-mediated tumor induction or the Apcmin/+ model were reviewed and approved by the Regierung Unterfranken and ethics committee under licenses 2532-2-555, 2532-2-556, 2532-2-694, and 2532-2-1002. The mouse strains used are detailed, and animals were maintained in standard cages under pathogen-free conditions, with a 12-hour light/dark cycle and free access to food and water, in compliance with FELASA2014 guidelines.

Experiments using AOM/DSS-induced colorectal tumors were approved by the Regierungspräsidium Darmstadt, Germany.

Human CRC tissue, regardless of donor sex, was obtained from the University Hospital Würzburg Pathology Department, with all patients providing informed consent. Experimental procedures followed the principles outlined in the WMA Declaration of Helsinki and the U.S. Department of Health and Human Services Belmont Report. Ethical approval for sample collection

was granted under protocol 17/01/2006 (University Hospital Würzburg).

The P6T human CRC organoids were established previously [31] and obtained under a material transfer agreement with Hubrecht Organoid Technology. Collection of colorectal tissue for organoid generation adhered to European Network of Research Ethics Committees (EUREC) standards, complying with European, national, and local legislation. Informed consent was obtained from all donors following ethical approval of the study protocols.

Acknowledgments: The Operetta High Content Microscope was funded by the Deutsche Forschungsgemeinschaft (DFG, German Research Foundation) -440766788 (INST 93/1023-1 -FUGG).

Conflict of Interest: None

Financial Support: MR is funded by the DKH MSNZ Wuerzburg, DFG-GRK 2243 and IZKF B335. OH is supported by the German Cancer Aid via grant 70112491 and 70114554. ME is supported by the TransOnc priority programme of the German Cancer Aid within grant 70112951 (ENABLE). AO and MED are funded by the German Israeli Foundation grant 1431 1431 and ICRF project grant to AO. AO, ID and MED are funded by the DIP-DFG grant DIP DI 931/18-1. ID and MED are funded by the DFG-TRR 387. Open Access funding enabled and organized by Projekt DEAL. HMM and CS are funded by the DFG (DFG MA6957/1-1).

Ethics Statement: None

References

1. Sung H, Ferlay J, Siegel RL, Laversanne M, Soerjomataram I, Jemal A, et al. Global Cancer Statistics 2020: GLOBOCAN Estimates of Incidence and Mortality Worldwide for 36 Cancers in 185 Countries. CA Cancer J Clin. 2021;71:209–49.
2. Risks and causes of bowel cancer. Cancer Research UK. https://www.cancerresearchuk.org/about-cancer/bowel-cancer/risks-causes.
3. Half E, Bercovich D, Rozen P. Familial adenomatous polyposis. Orphanet J Rare Dis. 2009;4:22.
4. Siegel RL, Miller KD, Fuchs HE, Jemal A. Cancer Statistics, 2021. CA Cancer J Clinicians. 2021;71:7–33.
5. Novellasdemunt L, Antas P, Li VS. Targeting Wnt signaling in colorectal cancer. A Review in the Theme: Cell Signaling: Proteins, Pathways and Mechanisms. Am J Physiol Cell Physiol. 2015;309:C511–521.
6. 6.Abu Ahmad Y, Oknin-Vaisman A, Bitman-Lotan E, Orian A. From the Evasion of Degradation to Ubiquitin-Dependent Protein Stabilization. Cells. 2021;10:2374.
7. Ranes M, Zaleska M, Sakalas S, Knight R, Guettler S. Reconstitution of the destruction complex defines roles of AXIN polymers and APC in beta-catenin capture, phosphorylation, and ubiquitylation. Mol Cell. 2021;81:3246–61.e3211.
8. Morin PJ, Sparks AB, Korinek V, Barker N, Clevers H, Vogelstein B, et al. Activation of beta-catenin-Tcf signaling in colon cancer by mutations in beta-catenin or APC. Science. 1997;275:1787–90.
9. Yang J, Zhang W, Evans PM, Chen X, He X, Liu C. Adenomatous polyposis coli (APC) differentially regulates beta-catenin phosphorylation and ubiquitination in colon cancer cells. J Biol Chem. 2006;281:17751–7.
10. Zhao H, Ming T, Tang S, Ren S, Yang H, Liu M, et al. Wnt signaling in colorectal cancer: pathogenic role and therapeutic target. Mol Cancer. 2022;21:144.
11. Zhan T, Rindtorff N, Boutros M. Wnt signaling in cancer. Oncogene. 2017;36:1461–73.
12. Hankey W, Frankel WL, Groden J. Functions of the APC tumor suppressor protein dependent and independent of canonical WNT signaling: implications for therapeutic targeting. Cancer Metastasis Rev. 2018;37:159–72.
13. Novellasdemunt L, Foglizzo V, Cuadrado L, Antas P, Kucharska A, Encheva V, et al. USP7 Is a Tumor-Specific WNT Activator for APC-Mutated Colorectal Cancer by Mediating beta-Catenin Deubiquitination. Cell Rep. 2017;21:612–27.
14. Barua D, Hlavacek WS. Modeling the effect of APC truncation on destruction complex function in colorectal cancer cells. PLoS Comput Biol. 2013;9:e1003217.
15. Schneikert J, Grohmann A, Behrens J. Truncated APC regulates the transcriptional activity of beta-

catenin in a cell cycle dependent manner. Hum Mol Genet. 2007;16:199–209.
16. Dominguez-Brauer C, Khatun R, Elia AJ, Thu KL, Ramachandran P, Baniasadi SP, et al. E3 ubiquitin ligase Mule targets beta-catenin under conditions of hyperactive Wnt signaling. Proc Natl Acad Sci USA. 2017;114:E1148–E1157.
17. Jiang JX, Sun CY, Tian S, Yu C, Chen MY, Zhang H. Tumor suppressor Fbxw7 antagonizes WNT signaling by targeting beta-catenin for degradation in pancreatic cancer. Tumour Biol. 2016;37:13893–902.
18. Chitalia VC, Foy RL, Bachschmid MM, Zeng L, Panchenko MV, Zhou MI, et al. Jade-1 inhibits Wnt signalling by ubiquitylating beta-catenin and mediates Wnt pathway inhibition by pVHL. Nat Cell Biol. 2008;10:1208–16.
19. Shearer RF, Iconomou M, Watts CK, Saunders DN. Functional Roles of the E3 Ubiquitin Ligase UBR5 in Cancer. Mol Cancer Res. 2015;13:1523–32.
20. Thomas JJ, Abed M, Heuberger J, Novak R, Zohar Y, Beltran Lopez AP, et al. RNF4-Dependent Oncogene Activation by Protein Stabilization. Cell Rep. 2016;16:3388–3400.
21. Gao C, Xiao G, Hu J. Regulation of Wnt/beta-catenin signaling by posttranslational modifications. Cell Biosci. 2014;4:13.
22. Chen C, Zhu D, Zhang H, Han C, Xue G, Zhu T, et al. YAP-dependent ubiquitination and degradation of beta-catenin mediates inhibition of Wnt signalling induced by Physalin F in colorectal cancer. Cell Death Dis. 2018;9:591.
23. Wu C, Luo K, Zhao F, Yin P, Song Y, Deng M, et al. USP20 positively regulates tumorigenesis and chemoresistance through beta-catenin stabilization. Cell Death Differ. 2018;25:1855–69.
24. Park HB, Kim JW, Baek KH. Regulation of Wnt Signaling through Ubiquitination and Deubiquitination in Cancers. Int J Mol Sci. 2020;21:3904.
25. Cerami E, Gao J, Dogrusoz U, Gross BE, Sumer SO, Aksoy BA, et al. The cBio cancer genomics portal: an open platform for exploring multidimensional cancer genomics data. Cancer Discov. 2012;2:401–4.
26. Gao J, Aksoy BA, Dogrusoz U, Dresdner G, Gross B, Sumer SO, et al. Integrative analysis of complex cancer genomics and clinical profiles using the cBioPortal. Sci Signal. 2013;6:pl1.
27. Ahmed Y, Hayashi S, Levine A, Wieschaus E. Regulation of armadillo by a Drosophila APC inhibits neuronal apoptosis during retinal development. Cell. 1998;93:1171–82.
28. van Neerven SM, de Groot NE, Nijman LE, Scicluna BP, van Driel MS, Lecca MC, et al. Apc-mutant cells act as supercompetitors in intestinal tumour initiation. Nature. 2021;594:436–41.
29. Flanagan DJ, Pentinmikko N, Luopajärvi K, Willis NJ, Gilroy K, Raven AP, et al. NOTUM from Apc-mutant cells biases clonal competition to initiate cancer. Nature. 2021;594:430–5.
30. Kumari N, Jaynes PW, Saei A, Iyengar PV, Richard JLC, Eichhorn PJA. The roles of ubiquitin modifying enzymes in neoplastic disease. Biochim Biophys Acta Rev Cancer. 2017;1868:456–83.
31. van de Wetering M, Francies HE, Francis JM, Bounova G, Iorio F, Pronk A, et al. Prospective derivation of a living organoid biobank of colorectal cancer patients. Cell. 2015;161:933–45.
32. Matano M, Date S, Shimokawa M, Takano A, Fujii M, Ohta Y, et al. Modeling colorectal cancer using CRISPR-Cas9-mediated engineering of human intestinal organoids. Nat Med. 2015;21:256–62.
33. Schulte C, Solda A, Spanig S, Adams N, Bekic I, Streicher W, et al. Multivalent binding kinetics resolved by fluorescence proximity sensing. Commun Biol. 2022;5:1070.
34. Martorell O, Merlos-Suarez A, Campbell K, Barriga FM, Christov CP, Miguel-Aliaga I, et al. Conserved mechanisms of tumorigenesis in the Drosophila adult midgut. PLoS One. 2014;9:e88413.
35. McCartney BM, Price MH, Webb RL, Hayden MA, Holot LM, Zhou M, et al. Testing hypotheses for the functions of APC family proteins using null and truncation alleles in Drosophila. Development. 2006;133:2407–18.
36. Higuchi M, Kawamura H, Matsuki H, Hara T, Takahashi M, Saito S, et al. USP10 Is an Essential Deubiquitinase for Hematopoiesis and Inhibits Apoptosis of Long-Term Hematopoietic Stem Cells. Stem Cell Rep. 2016;7:1116–29.
37. Schmitt M, Ceteci F, Gupta J, Pesic M, Bottger TW, Nicolas AM, et al. Colon tumour cell death causes mTOR dependence by paracrine P2X4 stimulation. Nature. 2022;612:347–53.
38. Watanabe S, Kobayashi S, Ogasawara N, Okamoto R, Nakamura T, Watanabe M, et al. Transplantation

of intestinal organoids into a mouse model of colitis. Nat Protoc. 2022;17:649–71.
39. O'Rourke KP, Loizou E, Livshits G, Schatoff EM, Baslan T, Manchado E, et al. Transplantation of engineered organoids enables rapid generation of metastatic mouse models of colorectal cancer. Nat Biotechnol. 2017;35:577–82.
40. Varga J, Nicolas A, Petrocelli V, Pesic M, Mahmoud A, Michels BE et al. AKT-dependent NOTCH3 activation drives tumor progression in a model of mesenchymal colorectal cancer. J Exp Med. 2020;217:e20191515.
41. Tian Y, Wang X, Cramer Z, Rhoades J, Estep KN, Ma X, et al. APC and P53 mutations synergise to create a therapeutic vulnerability to NOTUM inhibition in advanced colorectal cancer. Gut. 2023;72:2294–306.
42. Albuquerque C, Breukel C, van der Luijt R, Fidalgo P, Lage P, Slors FJ, et al. The 'just-right' signaling model: APC somatic mutations are selected based on a specific level of activation of the beta-catenin signaling cascade. Hum Mol Genet. 2002;11:1549–60.
43. Guren MG. The global challenge of colorectal cancer. Lancet Gastroenterol Hepatol. 2019;4:894–5.
44. Dewson G, Eichhorn PJA, Komander D. Deubiquitinases in cancer. Nat Rev Cancer. 2023;23:842–62.
45. Clague MJ, Urbe S, Komander D. Breaking the chains: deubiquitylating enzyme specificity begets function. Nat Rev Mol Cell Biol. 2019;20:338–52.
46. Li H, Li C, Zhai W, Zhang X, Li L, Wu B, et al. Destabilization of TP53 by USP10 is essential for neonatal autophagy and survival. Cell Rep. 2022;41:111435.
47. Yuan J, Luo K, Zhang L, Cheville JC, Lou Z. USP10 regulates p53 localization and stability by deubiquitinating p53. Cell. 2010;140:384–96.
48. Jia R, Bonifacino JS. The ubiquitin isopeptidase USP10 deubiquitinates LC3B to increase LC3B levels and autophagic activity. J Biol Chem. 2021;296:100405.
49. Liu J, Xia H, Kim M, Xu L, Li Y, Zhang L, et al. Beclin1 controls the levels of p53 by regulating the deubiquitination activity of USP10 and USP13. Cell. 2011;147:223–34.
50. Zhang M, Hu C, Tong D, Xiang S, Williams K, Bai W, et al. Ubiquitin-specific Peptidase 10 (USP10) Deubiquitinates and Stabilizes MutS Homolog 2 (MSH2) to Regulate Cellular Sensitivity to DNA Damage. J Biol Chem. 2016;291:10783–91.
51. Bhattacharya U, Neizer-Ashun F, Mukherjee P, Bhattacharya R. When the chains do not break: the role of USP10 in physiology and pathology. Cell Death Dis. 2020;11:1033.
52. Deng M, Yang X, Qin B, Liu T, Zhang H, Guo W, et al. Deubiquitination and Activation of AMPK by USP10. Mol Cell. 2016;61:614–24.
53. Hanahan D. Hallmarks of Cancer: New Dimensions. Cancer Discov. 2022;12:31–46.
54. Guo K, Ma Z, Zhang Y, Han L, Shao C, Feng Y, et al. HDAC7 promotes NSCLC proliferation and metastasis via stabilization by deubiquitinase USP10 and activation of beta-catenin-FGF18 pathway. J Exp Clin Cancer Res. 2022;41:91.
55. Wang Y, Mao A, Liu J, Li P, Zheng S, Tong T et al. USP10 strikes down beta-catenin by dual-wielding deubiquitinase activity and phase separation potential. Cell Chem Biol. 2023;30:1436–52.e10.
56. Saei A, Palafox M, Benoukraf T, Kumari N, Jaynes PW, Iyengar PV, et al. Loss of USP28-mediated BRAF degradation drives resistance to RAF cancer therapies. J Exp Med. 2018;215:1913–28.
57. Diefenbacher ME, Popov N, Blake SM, Schulein-Volk C, Nye E, Spencer-Dene B, et al. The deubiquitinase USP28 controls intestinal homeostasis and promotes colorectal cancer. J Clin Invest. 2014;124:3407–18.
58. Prieto-Garcia C, Hartmann O, Reissland M, Fischer T, Maier CR, Rosenfeldt M, et al. Inhibition of USP28 overcomes Cisplatin-resistance of squamous tumors by suppression of the Fanconi anemia pathway. Cell Death Differ. 2022;29:568–84.
59. Sun J, Li T, Zhao Y, Huang L, Sun H, Wu H, et al. USP10 inhibits lung cancer cell growth and invasion by upregulating PTEN. Mol Cell Biochem. 2018;441:1–7.
60. Lange SM, Armstrong LA, Kulathu Y. Deubiquitinases: From mechanisms to their inhibition by small molecules. Mol Cell. 2022;82:15–29.
61. Weisberg EL, Schauer NJ, Yang J, Lamberto I, Doherty L, Bhatt S, et al. Inhibition of USP10 induces degradation of oncogenic FLT3. Nat Chem Biol. 2017;13:1207–15.